

N O T I C E

THIS DOCUMENT HAS BEEN REPRODUCED FROM
MICROFICHE. ALTHOUGH IT IS RECOGNIZED THAT
CERTAIN PORTIONS ARE ILLEGIBLE, IT IS BEING RELEASED
IN THE INTEREST OF MAKING AVAILABLE AS MUCH
INFORMATION AS POSSIBLE

| | | | | | |
|---|--|---|---|--|------------------------------|
| 1. REPORT NO. NASA TM -86523 | | 2. GOVERNMENT ACCESSION NO. | | 3. RECIPIENT'S CATALOG NO. | |
| 4. TITLE AND SUBTITLE Test Method for Telescopes Using a Point Source at a Finite Distance, Center Director's Discretionary Fund Final Report, Project No. H20 | | | | 5. REPORT DATE September 1985 | |
| | | | | 6. PERFORMING ORGANIZATION CODE | |
| 7. AUTHOR(S) Donald B. Griner, E. Zissa, and Dietrich Korsch* | | | | 8. PERFORMING ORGANIZATION REPORT # | |
| 9. PERFORMING ORGANIZATION AND ADDRESS George C. Marshall Space Flight Center Marshall Space Flight Center, Alabama 35812 | | | | 10. WORK UNIT NO. | |
| | | | | 11. CONTRACT OR GRANT NO. | |
| | | | | 13. TYPE OF REPORT & PERIOD COVERED Technical Memorandum | |
| 12. SPONSORING AGENCY NAME AND ADDRESS National Aeronautics and Space Administration Washington, D.C. 20546 | | | | 14. SPONSORING AGENCY CODE | |
| 15. SUPPLEMENTARY NOTES Prepared by Information and Electronic Systems Laboratory, Science and Engineering Directorate. * Korsch Optics, Inc. | | | | | |
| 16. ABSTRACT <p>A test method for telescopes that makes use of a focused ring formed by an annular aperture when using a point source at a finite distance was evaluated theoretically and experimentally. The results show that the concept can be applied to near-normal as well as grazing incidence. It is particularly suited for x-ray telescopes because of their intrinsically narrow annular apertures, and because of the largely reduced diffraction effects.</p> | | | | | |
| 17. KEY WORDS Optical Testing Test Methods X-Ray Telescopes Optical Telescopes AXAF Ring Focus | | | 18. DISTRIBUTION STATEMENT Unclassified - Unlimited | | |
| 19. SECURITY CLASSIF. (of this report) Unclassified | | 20. SECURITY CLASSIF. (of this page) Unclassified | | 21. NO. OF PAGES 22 | 22. PRICE NTIS |

ACKNOWLEDGMENTS

The authors would like to thank J. D. Schaefer of the Information and Electronic Systems Laboratory for his assistance in taking and developing the series of photographs through the focused ring and best point image.

TABLE OF CONTENTS

| | Page |
|---|------|
| SUMMARY | 1 |
| INTRODUCTION | 1 |
| NUMERICAL EVALUATION OF EXAMPLES OF X-RAY TELESCOPES | 4 |
| LABORATORY DEMONSTRATION OF EXAMPLES OF VISIBLE TELESCOPES | 6 |
| CONCLUSIONS AND RECOMMENDATIONS | 13 |
| REFERENCES | 17 |

LIST OF ILLUSTRATIONS

| Figure | Title | Page |
|--------|--|------|
| 1. | Ring deformations due to misalignments | 2 |
| 2. | Intensity shift due to misalignments | 3 |
| 3. | Schematic of image space geometry..... | 4 |
| 4. | Schematic of laboratory test system..... | 7 |
| 5. | Parameters of laboratory test system..... | 7 |
| 6. | View of test system toward telescope entrance aperture | 8 |
| 7. | View of test system toward telescope exit aperture..... | 9 |
| 8. | Calculated intensity distribution at the ring focus of the test system at 1/8th scale | 10 |
| 9. | Series of photographs from before the ring focus through the best point image..... | 11 |
| 10. | Blow-up of focused ring (frame 3 of Fig. 9)..... | 12 |
| 11. | Blow-up of best point image (frame 10 of Fig. 9) | 14 |
| 12. | Cross section of a similar focused ring by the pinhole scanner..... | 15 |
| 13. | Schematic of small Cassegrain telescope designed to demonstrate the variation of the focused ring with misalignments | 16 |
| 14. | Parameters of small Cassegrain telescope designed to demonstrate the variation of the focused ring with misalignments | 16 |

TECHNICAL MEMORANDUM

TEST METHOD FOR TELESCOPES USING A POINT SOURCE AT A FINITE DISTANCE

MSFC Center Director's Discretionary Fund
Final Report, Project No. H20

SUMMARY

A test method for telescopes that makes use of a focused ring formed by an annular aperture when using a point source at a finite distance was evaluated theoretically and experimentally. The High Resolution Mirror Assembly (HRMA) and the Technology Mirror Assembly (TMA) both of the Advanced X-ray Astrophysics Facility (AXAF) projects were used as models for the theoretical analysis of grazing-incidence systems, and a one-sixth spherical-mirror version of the Hubble Space Telescope (HST) served as a model for near-normal incidence systems. The existence of a sharply focused ring was demonstrated experimentally using the existing HST model with a point source and an annular entrance aperture. The results show that the concept can be applied to near-normal as well as grazing incidence. It is particularly suited for x-ray telescopes because of their intrinsically narrow annular apertures, and because of the largely reduced diffraction effects.

INTRODUCTION

Testing a large aperture telescope is difficult because it requires a high precision collimator that produces a beam the diameter of which is as large as the aperture of the telescope. Furthermore, the quality of the test collimator must be equal to or better than the expected quality of the telescope itself. This frequently causes a problem, particularly with large, high resolution grazing-incidence telescopes. Attempts to test a telescope with a point-like source at a finite distance often fails because the finite object distance introduces a sufficient amount of spherical aberration in the telescope to prohibit resolution measurements to the required accuracy. However, it is also that very same spherical aberration that provides the opportunity for an alternative method to test the quality of the telescope [1].

If an axially symmetric system is illuminated by an on-axis point source through a narrow annular aperture, then, in the presence of spherical aberration, a sharply focused ring is formed in front of or behind the best-focus image plane, depending on the amount and the sign of the spherical aberration. Any deviation from circular symmetry as well as changes in the thickness of the ring are indications of surface defects and alignment errors in the imaging system and may be analyzed as such. Typical ring deformations caused by an off-axis point source, a tilted, and a decentered secondary mirror in a two-mirror system are shown in Figure 1. Severe ring deformations as shown are caused by substantial misalignments. In addition to the global deformation there is a redistribution of the intensity along the perimeter of the ring that is measurable even before any visible sign of a deformation appears. This effect can be used to detect very small amounts of alignment errors. An example of this intensity shift due to a small amount of misalignment is shown in

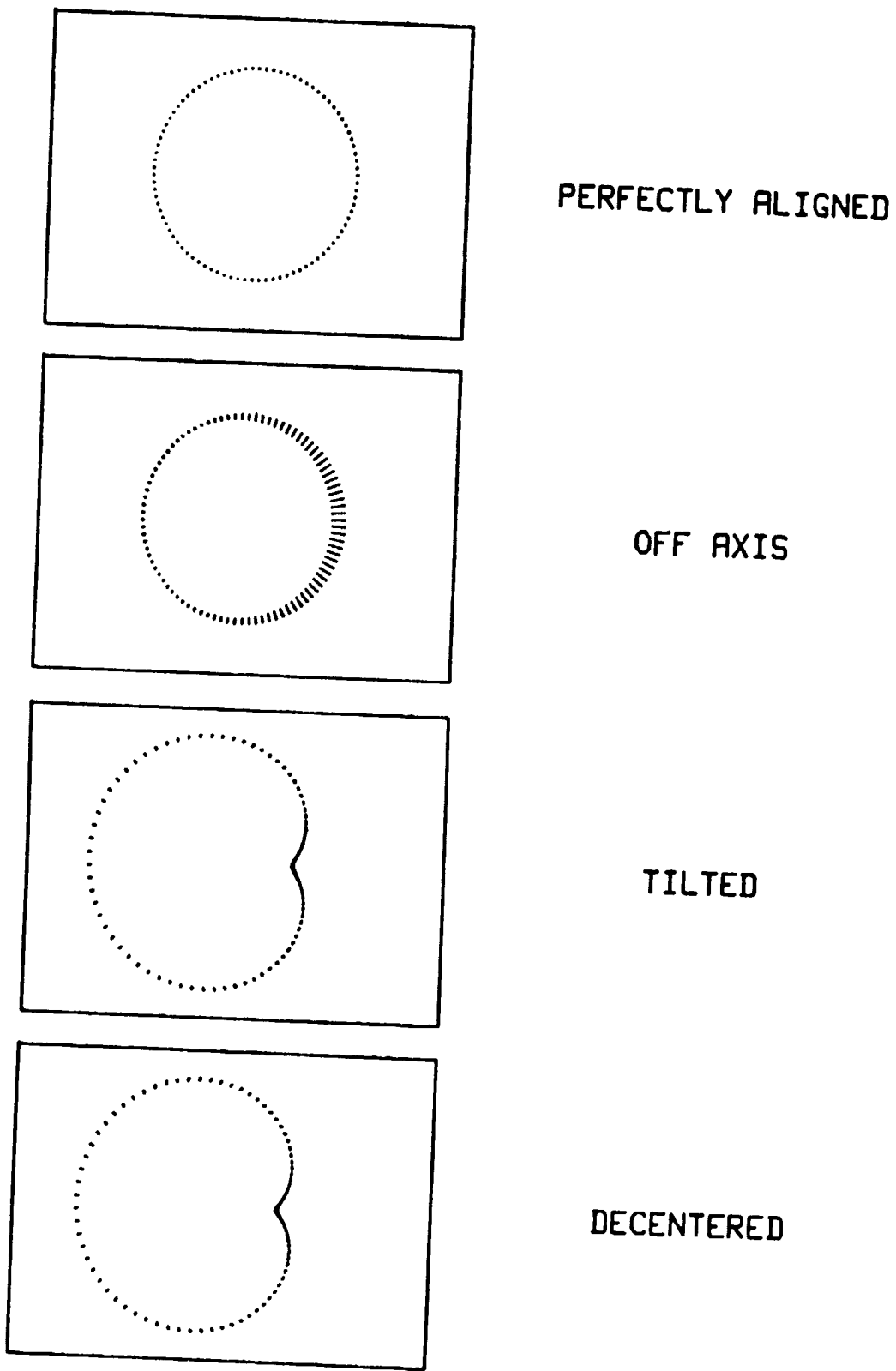


Figure 1. Ring deformations due to misalignments.

Figure 2. To optimize the measurement accuracy, the focused ring should be as thin as possible. According to geometrical optics, the width of the ring decreases with the width of the entrance annulus. There is, however, a counteracting effect due to diffraction which causes a broadening of the ring that is proportional to the wavelength and inversely proportional to the width of the annulus. Both effects must be taken into account when minimizing the width of the ring.

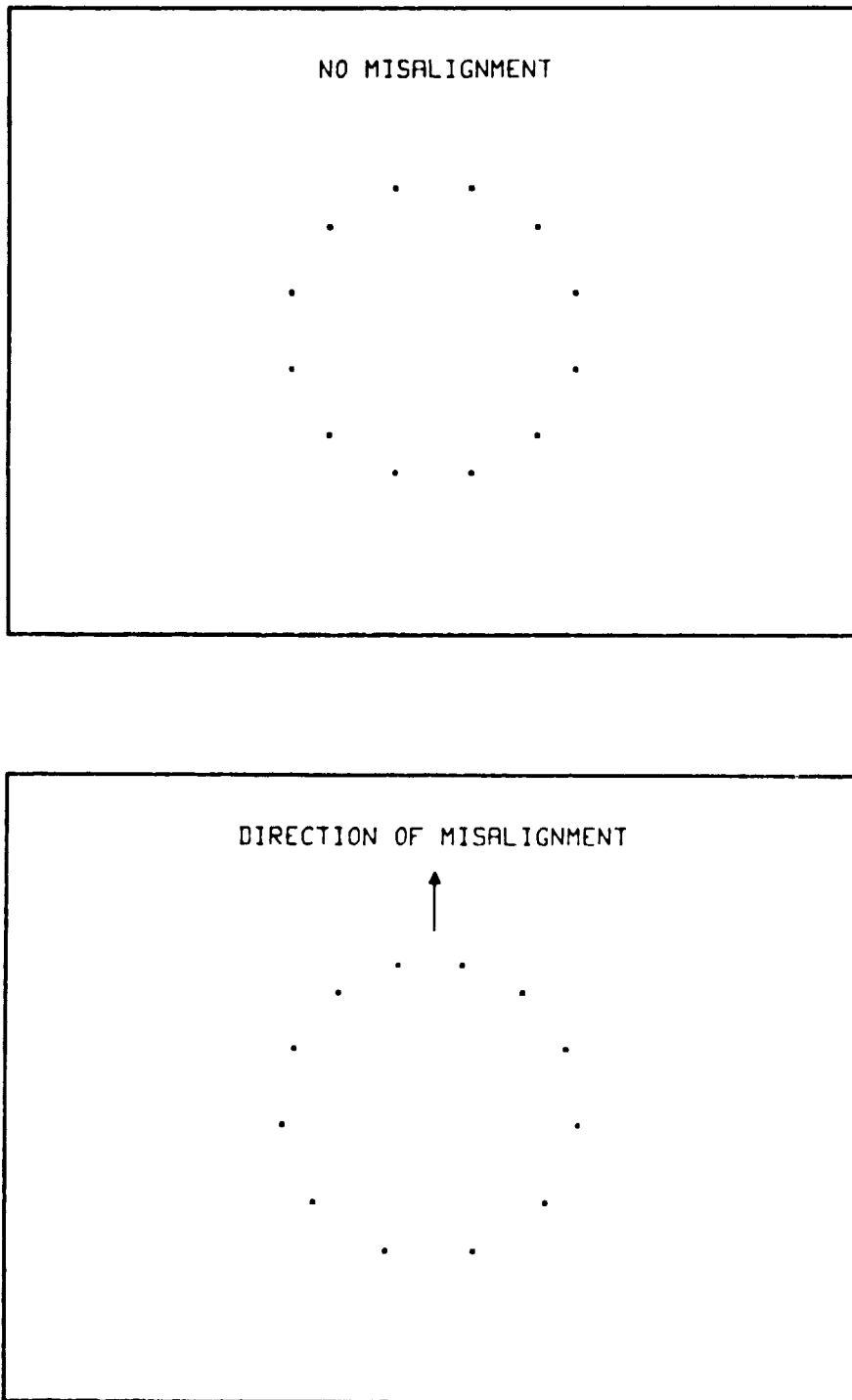


Figure 2. Intensity shift due to misalignments.

While the focused ring and its reactions to alignment errors and surface defects are observed in both near-normal and grazing-incidence systems, the grazing-incidence telescope is a more natural candidate for this test procedure because of its inherently narrow entrance aperture, and because it produces only a minimal diffraction effect due to the shortness of x-ray wavelengths.

NUMERICAL EVALUATION OF EXAMPLES OF X-RAY TELESCOPES

Two specific x-ray telescopes were evaluated numerically in order to examine the ring focus. The AXAF High Resolution Mirror Assembly was examined in terms of the position and size of the focused rings as well as their sensitivity to alignment errors. The position and size of the focused ring was also calculated for the AXAF Technology Mirror Assembly.

It was the particular problems associated with testing the AXAF telescope using a point source at a finite distance that stimulated the development of this test method. The spherical aberration introduced by an object distance of about 1000 ft, the maximum allowed by the presently existing test tunnel, precludes a resolution measurement to the desired accuracy when using the best point image. A test using the sharply focused ring image which is located between the focal plane for an infinite object distance and the best point image plane for a finite object distance was, therefore, suggested.

The dimensions related to the image space geometry which is schematically depicted in Figure 3 were obtained by exact ray tracing and are summarized in Table 1 for all six subsystems. The best point image and the ring focus locations are

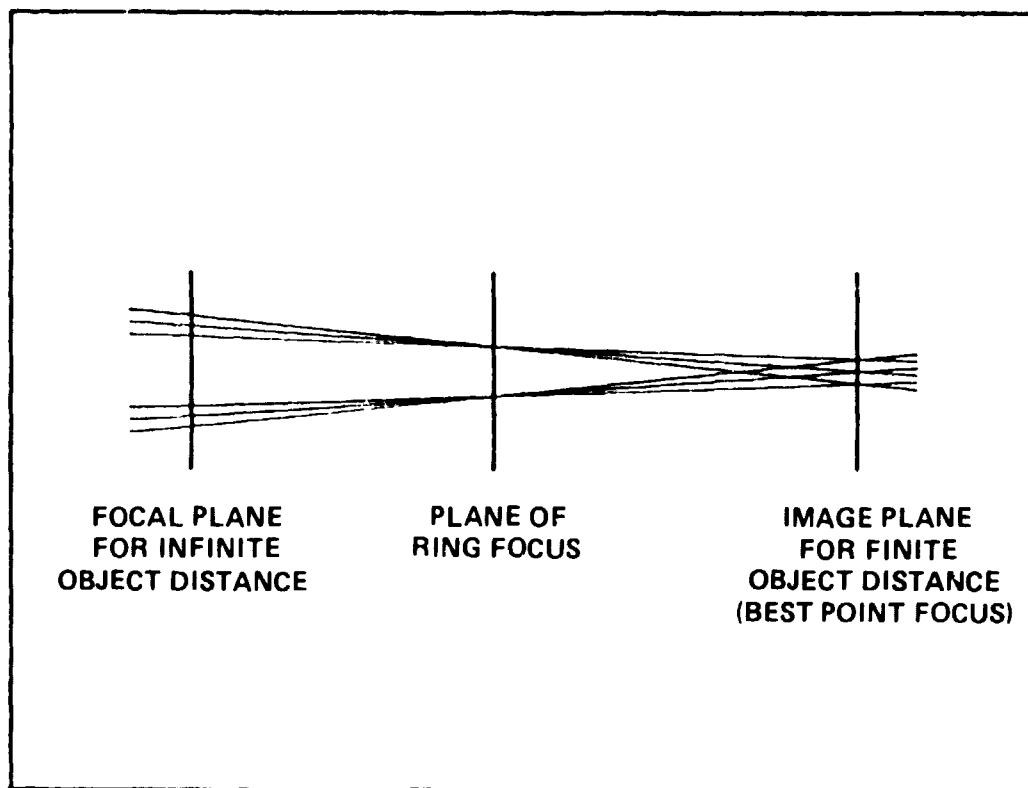


Figure 3. Schematic of image space geometry.

**TABLE 1. IMAGE SPACE DIMENSIONS OF THE SIX AXAF SUBSYSTEMS
IN THE PRESENCE OF SPHERICAL ABERRATION AND
AN OBJECT DISTANCE OF 1000 ft**

| | I | II | III | IV | V | VI |
|---------------------------------------|--------|--------|--------|--------|--------|--------|
| Best Focus Location (in.) | 13.545 | 13.553 | 13.560 | 13.565 | 13.570 | 13.574 |
| Ring Image Location (in.) | 5.478 | 5.454 | 5.433 | 5.414 | 5.399 | 5.385 |
| Ring Diameter (in.) | 0.939 | 0.852 | 0.760 | 0.674 | 0.588 | 0.502 |
| Best Focus Spot Diameter (μ rad) | 25 | 23 | 20 | 18 | 16 | 13 |
| Ring Width (μ rad) | 0.43 | 0.39 | 0.35 | 0.31 | 0.27 | 0.23 |

measured from the telescope focal plane for an infinitely distant object. The numbers for the ring focus locations indicate that all six rings are located essentially in the same plane. A comparison in size of the diameter of the best point image and the width of the focused ring clearly shows the advantage of the ring which is almost two orders of magnitude sharper than the point image.

The allowable errors for the AXAF telescope are so small that one would have to make use of intensity redistribution effect, as shown in Figure 2, to make the measurements. The intensity shift along the perimeter of the ring occurs such that maximum and minimum intensities appear at opposite sides along the direction of the misalignment. Special aperture configurations may be used to facilitate the measurement of this effect. If, for instance, the entrance aperture is masked to create a series of equidistant radial slits, the continuous ring will be replaced by a series of circularly arranged focused spots. A secondary tilt or decenter then causes a change in the distance between these spots as indicated in Figure 2. If the distance between the slits corresponds to 30 deg, the difference of the maximum and minimum linear distances between adjacent spots is, interestingly, for all six subsystems the same, and amounts to the following:

19.5 microns per microradian tilt,

or

9.6 microns per 10 micron decenter .

Furthermore, since in the case of nested grazing-incidence telescope systems each subsystem forms its own focused ring, the concentricity of these rings is a good indication of the state of their axial alignment.

The focused ring test would also be a valuable supplement to tests planned for Technology Mirror Assembly (TMA). The TMA is a 16-in.-diameter test model of an x-ray mirror pair and its construction demonstrates the technology needed to

build AXAF. For a 1000-ft source distance, an exact ray trace showed that the focused ring would be 2.9 mm in diameter and would be located 1.6 in. in front of the best point image. Thus, it would be close to the instruments set up to measure the best point image.

LABORATORY DEMONSTRATION OF EXAMPLES OF VISIBLE TELESCOPES

This section reports on the laboratory demonstration of the focused ring with the 1/6th scale model of Hubble Space Telescope (HST) as well as the plans to construct a small Cassegrain telescope specifically designed to show the effects of misalignments. Normal-incidence visible-light telescopes are used for demonstration for practical reasons.

The 1/6th scale model which had been used to test a straylight suppression system for HST was found to be suitable for a first look at the ring focus effect in the visible region. A schematic of the source and telescope is shown in Figure 4. The parameters of the system are given in Figure 5. Photographs of the system are shown in Figures 6 and 7. The ring focus effect was enhanced by the telescope model's large spherical aberration caused by both of its mirrors being spherical. The annular aperture was added near the outside edge of the telescope. This resulted in a ring focus which was well separated from the best point focus even for an infinite source distance. The width of the annulus was chosen large enough to insure that the diffractive width at the focused ring was not large compared to the geometric width. The light bundle was made to diverge slightly at the telescope aperture in order to put the ring focus and best point image at easily accessible points behind the telescope.

Exact ray trace calculations showed that if the pinhole of the source were placed 5 in. inside of the focus of the parabolic collimator, the focused ring would have a diameter of 12.6 mm and would be located 15.4 in. behind the exit aperture of the telescope. Under the same conditions the best point image would be located 24.7 in. behind the telescope exit aperture. The rms geometric width of the focused ring would be 230 microns. The distance between the first minima on either side of a single slit diffraction pattern from the width of the annular aperture would be 106 microns for a wavelength of 632.8 nm. These widths are small compared to the 1670 micron geometric rms diameter of best point focus. This implied that there would be an easily observable minimum ring width before the best point image. An intensity distribution at the ring focus was determined including diffraction effects. The available computer only allowed calculation of the system in Figures 4 through 7 at 1/8th scale. The results are shown in Figure 8. In addition to the ring there is also a central maximum due to diffraction. Also there are straight lines due to diffraction off the support spiders of the telescope aperture plate. Although the latter effects may be difficult to see in Figure 8, they can be seen in photographs shown below.

The images of the system were recorded both with a 35 mm camera without lenses and a pinhole scanner. Figure 9 shows a series of photographs from before the ring focus through the best point image. Although the source distance was not exactly the same as in the calculations above, the pictures show all of the effects mentioned above. The deviations from circular symmetry may be due to misalignments in the system. The ring focus is near frame number 3 and the best point image is near frame number 10 in Figure 9. A blow-up of the focused ring is in Figure 10 to show the diffractive ring structure. The diameter of the outside edge of the ring

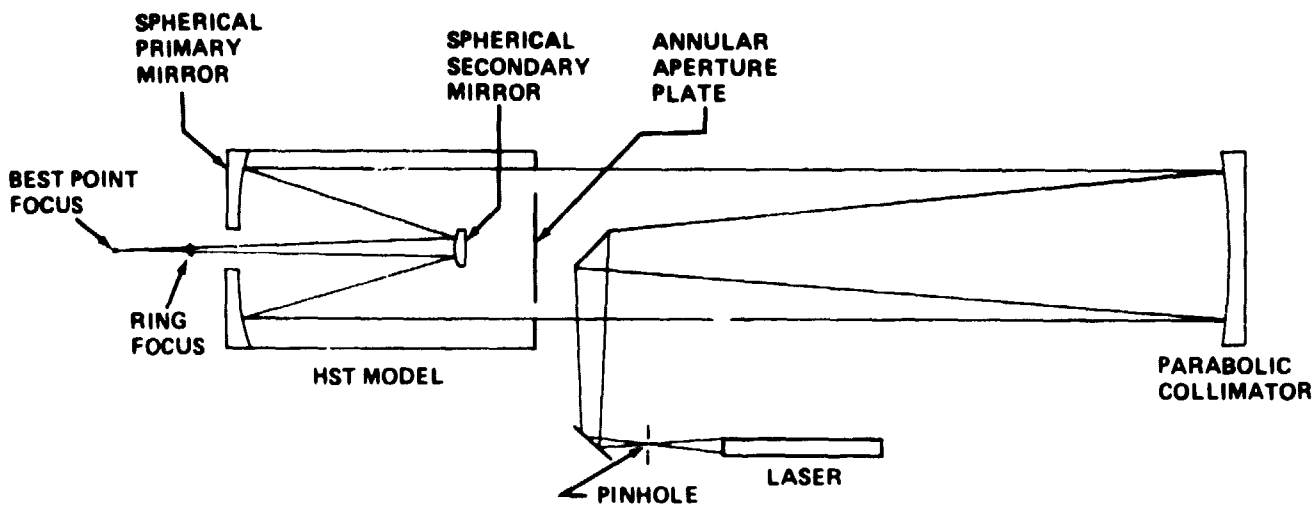


Figure 4. Schematic of laboratory test system.

Spherical Primary Mirror:

Radius of Curvature: -2.2 m.
 Diameter: 0.5 m.
 Hole in center: 5.0 in. diameter

Spherical Secondary Mirror:

Radius of Curvature: -0.54 m.
 Diameter: 0.11 m.

Annular Aperture Plate

Inner radius: 6 in.
 Outer radius: 9 in.

Parabolic Collimator

Diameter: 20 in.
 Focal length: 140 in.

Spacing

Collimator to Aperture Plate: 12 ft.
 Aperture Plate to Primary Mirror: 46.5 in.
 Primary to Secondary Mirror: 34.6 in.

Pinhole Source

Wavelength: 632.8 nm.

Figure 5. Parameters of laboratory test system.

ORIGINAL PAGE IS
OF POOR QUALITY

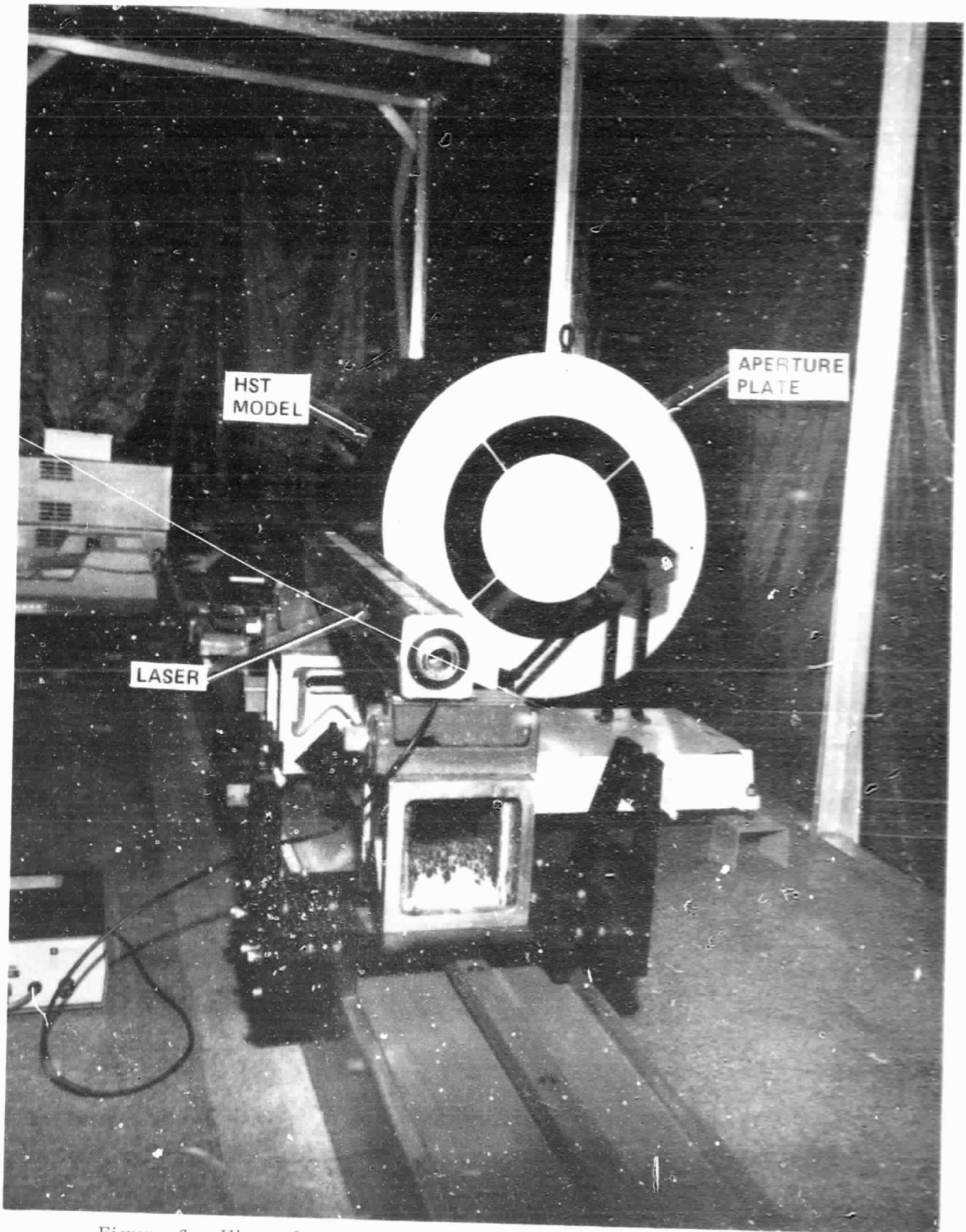


Figure 6. View of test system toward telescope entrance aperture.

ORIGINAL DOCUMENT
OF POOR QUALITY

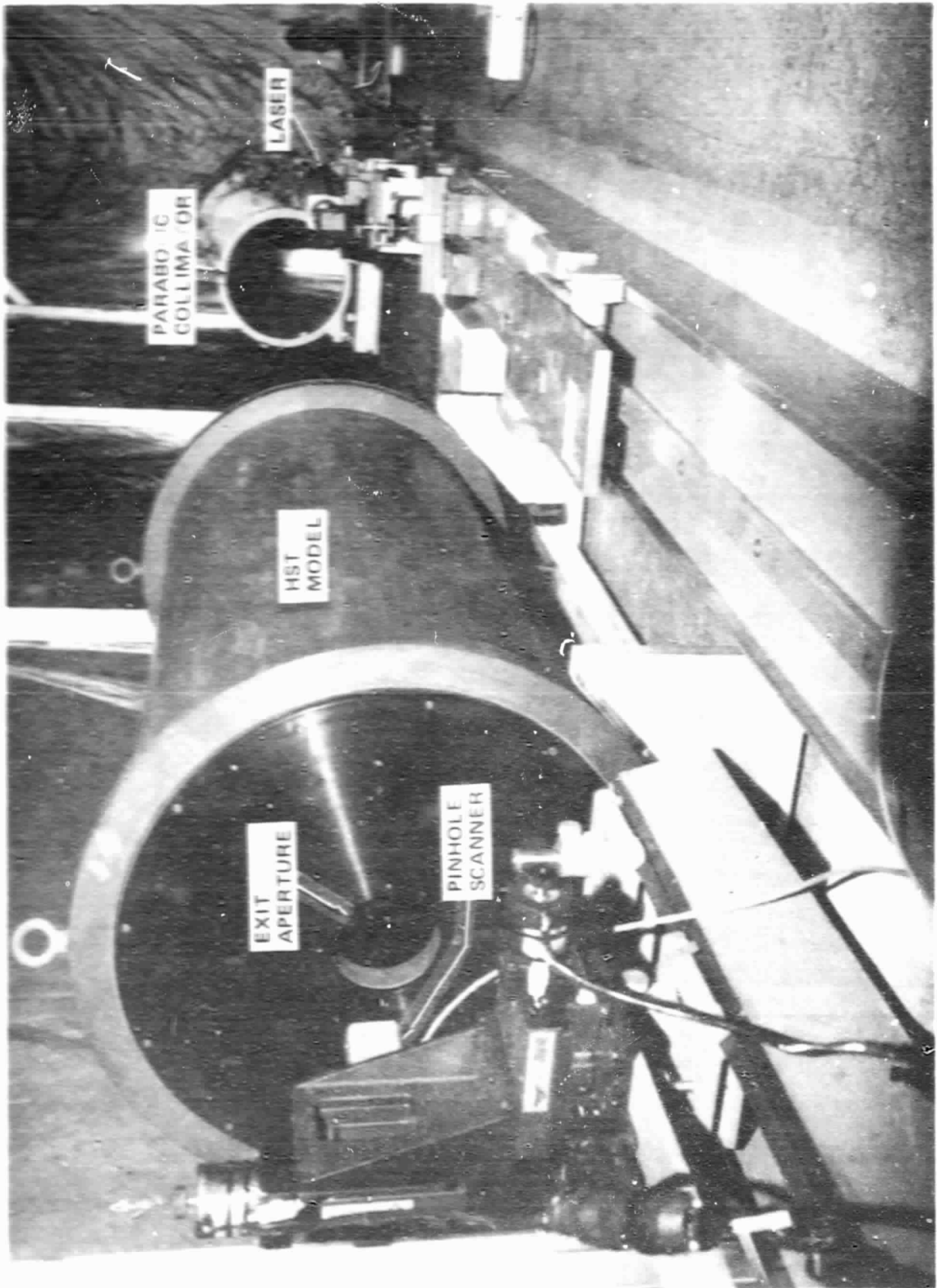


Figure 7. View of test system toward telescope exit aperture.

ORIGINAL [unclear]
OF POOR QUALITY

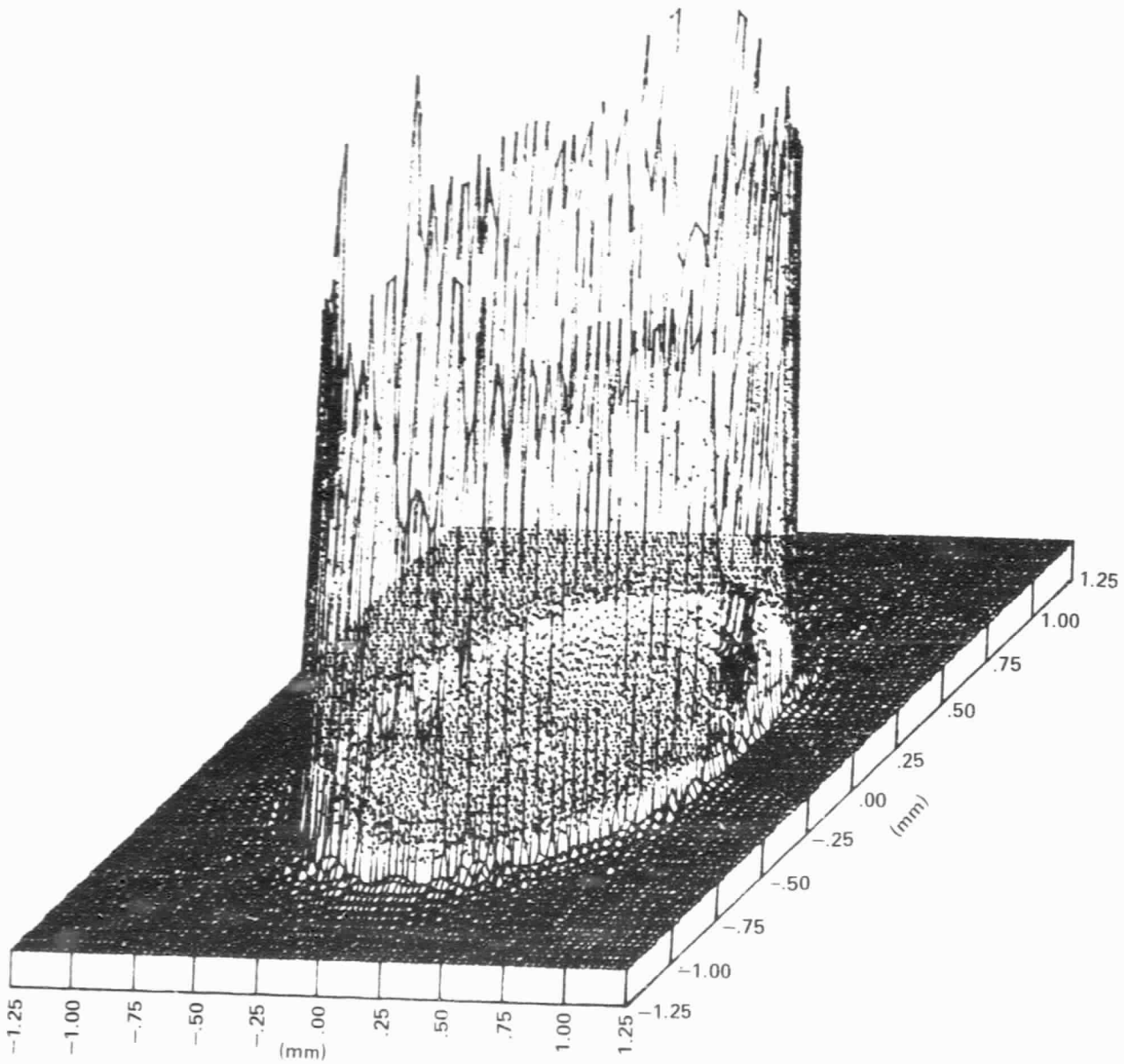


Figure 8. Calculated intensity distribution at the ring focus of the test system at 1/8th scale.

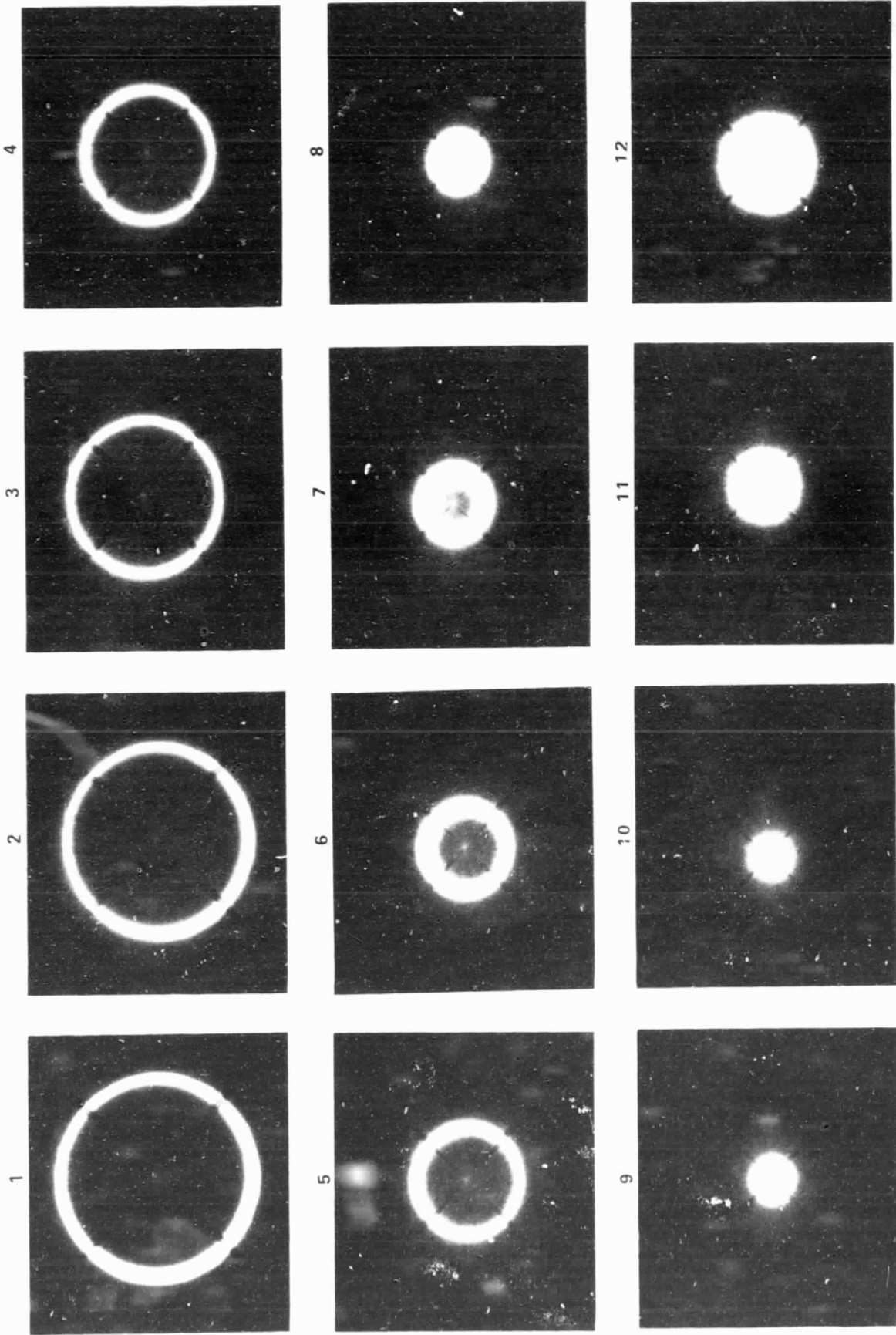


Figure 9. Series of photographs from before the ring focus through the best point image.

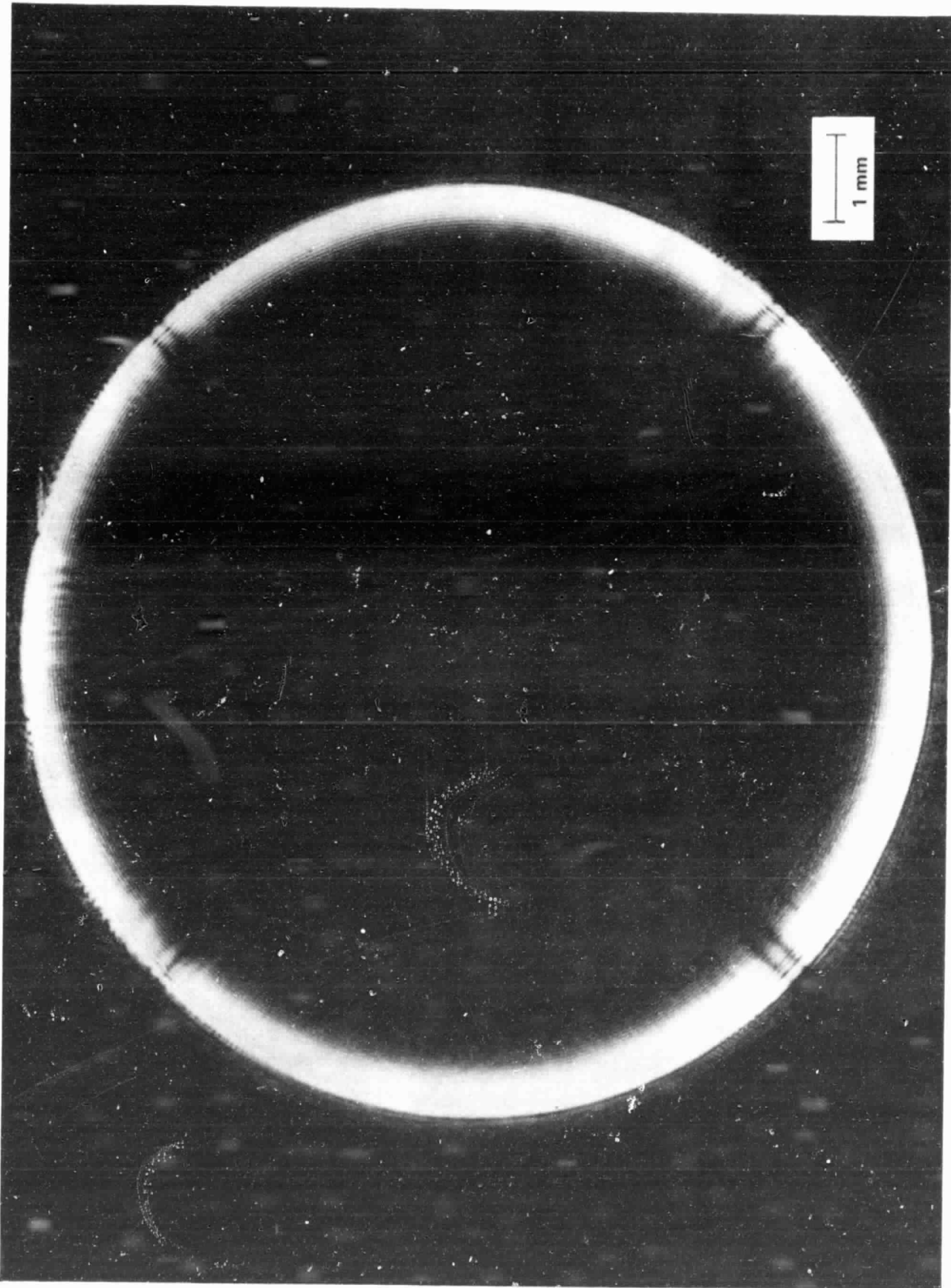


Figure 10. Blow-up of focused ring (frame 3 of Fig. 9).

is about 11 mm. Most of the energy in the ring is at the outside edge. Figure 11 is a blow-up of the best point image with the same magnification as Figure 10.

Figure 12 shows a cross section of a similar focused ring as seen by the pinhole scanner. This also shows the diffractive ring structure discussed above. The pinhole scanner consisted of a photodiode behind a 10 micron hole. This detector was mounted on a three-axis motorized translater with 1 micron resolution. The pinhole scanner output can be directly digitized and stored for analysis. It is planned to make a series of whole images with the scanner similar to the above photographs. One problem is how to deal with the large changes in intensity through the series of scans. A possible solution to this is to use the photodiode in a logarithmic mode.

Physical constraints of this particular system did not allow demonstration of the variation of the focused ring with misalignments. Figure 13 shows the schematic of a small Cassegrain telescope designed for this purpose. Figure 14 gives the parameters of the proposed visible light system.

CONCLUSIONS AND RECOMMENDATIONS

A new method to test telescopes using a point source at a finite distance was evaluated. The existence of a sharply focused ring formed by a telescope with a narrow annular aperture when illuminated by an axial point source at a finite distance was theoretically predicted and experimentally verified. The influence of various alignment errors on the shape of the ring was analyzed for several telescope models representing near-normal and grazing-incidence systems. While the validity of the test principle has been established during this phase of the study, further experiments will be necessary to quantitatively relate measurable observations to actual alignment errors and surface inaccuracies. To this end it is strongly recommended to perform a series of measurements using a test telescope especially designed and built to allow the introduction of known alignment errors. For practical purposes, this telescope should work in near-normal incidence using a visible light source. The design of such a telescope has been presented.

In addition it would seem very useful to supplement the tests already performed on the TMA by a further test using the method described here.

ORIGINAL
OF POOR QUALITY



Figure 11. Blow-up of best point image (frame 10 of Fig. 9).

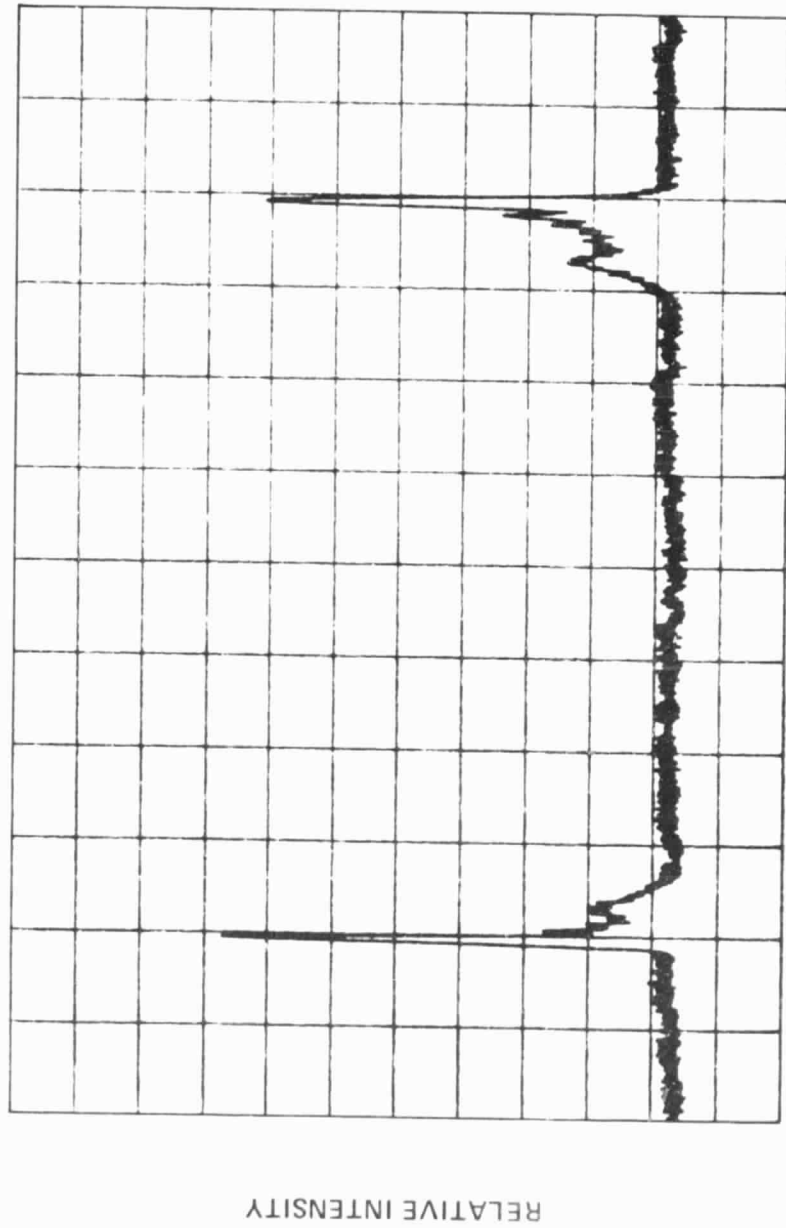


Figure 12. Cross section of a similar focused ring by the pinhole scanner.

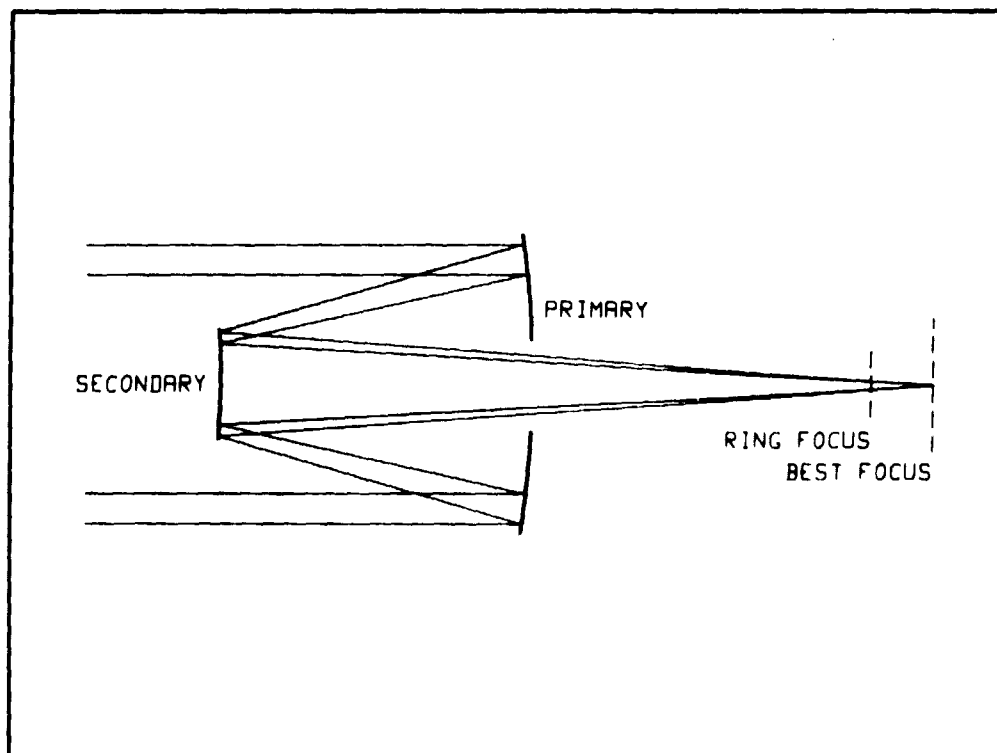


Figure 13. Schematic of small Cassegrain telescope designed to demonstrate the variation of the focused ring with misalignments.

Primary

Shape: Spherical
 Radius of Curvature: -400 mm.
 Diameter: 120 mm.

Secondary

Shape: Spherical
 Radius of Curvature: -200 mm.
 Diameter: 50 mm.

Spacing

Primary to Secondary: 125 mm.
 Secondary to Best Focus: 285 mm.

Figure 14. Parameters of small Cassegrain telescope designed to demonstrate the variation of the focused ring with misalignments.

REFERENCES

1. Korsch, D.: Design and Analysis in Support of AXAF. Final Report to MSFC, Contract NAS8-35622, April 1985.

APPROVAL

TEST METHOD FOR TELESCOPES USING A POINT SOURCE
AT A FINITE DISTANCE

MSFC Center Director's Discretionary Fund
Final Report, Project No. H20

By Donald B. Griner, David E. Zissa, and Dietrich Korsch

The information in this report has been reviewed for technical content. Review of any information concerning Department of Defense or nuclear energy activities or programs has been made by the MSFC Security Classification Officer. This report, in its entirety, has been determined to be unclassified.

W. C. Bradford

W. C. BRADFORD
Director, Information and Electronic
Systems Laboratory